Optimization of sulfuric acid hydrolysis conditions for preparation of nanocrystalline cellulose from enzymatically pretreated fibers

Beltramino, Facundo; Roncero, M. Blanca*; Vidal, Teresa; Valls, Cristina

CELBIOTECH_Paper Engineering Research Group. Universitat Politècnica de Catalunya (UPC. BarcelonaTech). Colom 11, E-08222, Terrassa, Spain.

Correspondence at all stages of refereeing and publication to:

Facundo Beltramino

CELBIOTECH_Paper engineering research group. Universitat Politècnica de Catalunya (UPC. BarcelonaTech). Colom 11, E-08222, Terrassa, Spain.

Email: facundo.beltramino@etp.upc.edu; Tel.: +34 937 398 190, Fax: +34 937 398 101

Correspondence to post-publication to:

M. Blanca Roncero

CELBIOTECH_Paper engineering research group. Universitat Politècnica de Catalunya (UPC. BarcelonaTech). Colom 11, E-08222, Terrassa, Spain.

Email: roncero@etp.upc.edu; Tel.: +34 937 398 210, Fax: +34 937 398 101

Keywords

Nanocrystalline cellulose; Cellulose nanocrystals; Optimization; Cellulase; Enzymatic treatment; Yield increase

Abstract

NCC preparation using sulfuric acid hydrolysis from cellulase pretreated fibers was optimized in order to obtain the highest possible yield with 62% and 65% wt. sulfuric acid throughout two statistical plans. At optimal conditions (10U/g odp cellulase, 25 min hydrolysis, 47 ºC and 62 % wt. H_2SO_4) high yields were obtained (≥80%) including an increase produced by enzyme of ~9 %. Optimal conditions produced nanosized particles of around ~200 nm with a reduced surface charge and sulfur content. The performed optimization allowed reducing the hydrolysis time in a 44%, and also increasing yield in more than 10% compared to results exposed in previous works. The effects of cellulase pretreatment were noticeable even under aggressive hydrolysis conditions, emphasizing its possibilities. Zeta potential and polydispersity indexes indicated that all studied conditions leaded to good quality final products, with values among -50 mV and 0.2, respectively. TEM analysis confirmed the presence of NCC and suggested morphological differences between samples. Finally FTIR analysis provided evidence that cellulase treatment

increased crystallinity of both cellulose fibers and NCC, and also increased accessibility to fibers, supporting data obtained from NCC.

Abbreviations

C > Cellulase-treated fibers

C_NCC > NCC obtained from cellulase pretreated fibers

CMC > Carboxymethil cellulose

FTIR > t transformed infrared spectroscopy

KC > Control fibers

KC_NCC > NCC obtained from control fibers

NCC > Nanocrystalline cellulose

Opd > Oven-dried pulp

LOI > Lateral order index

TCI > Total crystallinity index

U > Enzymatic activity unit

Introduction

During the last decades, human activities and their increasing energetic demand leaded to an overuse of non-renewable resources such as coal, petroleum or natural gas, which produced a dramatic increment in the pollution generated by these activities (Flauzino Neto et al. 2013). In this scenario of growing environmental concern, a shift in our society towards the use of natural renewable resources to fulfill our necessities was produced (Flauzino Neto et al. 2013). Cellulose, being one of the most important natural polymers on earth and virtually inexhaustible is a key source of sustainable materials suitable for industrial applications (Klemm et al. 2011).

Physically, cellulose is a fibrous, tough, water-insoluble substance that plays an essential role in maintaining the structure of plant cell walls (Habibi et al. 2010). Chemically, cellulose consists on a linear homopolymer of β-D-glucopyranose units linked by glycosidic bonds, while its repeating subunit consists of two glucose units linked corkscrewed 180º respect each other (Habibi et al. 2010). Cellulose chains aggregate onto larger structures, *i.e.* microfibrils. These microfibrils present a crystalline ordering which is disrupted by amorphous regions. Degradation of these defects leads to the release of needle-like particles consisting of crystalline regions, denominated nanocrystalline cellulose (NCC) or cellulose nanocrystals (CNC) (Habibi et al. 2010). The interest in NCC lies in that it presents outstanding mechanical properties at the nano-scale, making it a very interesting sustainable reinforcing agent for a variety of materials (Klemm et al. 2011). NCC chemical properties, which strongly depend of the preparation method used, determine their physicochemical behavior when incorporated onto polymeric matrixes or other composites (Klemm et al. 2011). Applications for NCC include: improvement of mechanical properties, modification of thermal properties, modification of barrier properties of nanocomposites, optical properties control, and potential uses in biomedicine (Brinchi et al. 2013).

In literature, isolation of NCC has been carried out by diverse methods, which have traditionally been characterized by low yields, reducing their economic and environmental efficiency. Studies such as those reported by Fan and Li (2012) and Chen et al. (2015) addressed this topic studying ways to increase sulfuric acid hydrolysis yield, the most extended preparation method. Other methods, such as NCC preparation through enzymatic hydrolysis of cellulose in combination with chemical and/or mechanical treatments have also been proposed by some authors (Filson et al. 2009; Anderson et al. 2014; Teixeira et al. 2015). These methods usually lead to very low yields and also to uncharged particles producing unstable suspensions, reducing their industrial interest. Previous studies from our group (Beltramino et al. 2015a) demonstrated that the combination of an enzymatic pretreatment with sulfuric acid hydrolysis could increase the yield of NCC isolation while influencing other properties and leading to well-stable suspensions of electrically charged nanoparticles. Hence, the introduction of biotechnology would improve the efficiency of this isolation as well as it would permit to reduce the environmental impact of sulfuric acid hydrolysis. In a previous work, we observed that the noticeability of enzymatic pretreatment effects on NCC is largely dependent on the hydrolysis conditions used for isolation. Experimental designs have been used in literature in order to optimize process conditions (Valls and Roncero 2009; Valls et al. 2010). In this work, two experimental plans were carried out with two different acid doses in order to study the influence of three variables: the presence of an enzymatic pretreatment, hydrolysis time and hydrolysis temperature on NCC preparation. To our best knowledge, an optimization of this kind was being performed on enzymatically pretreated fibers for the first time. The aim of this work was to both maximize NCC yield from enzymatically pretreated fibers and also to assess the relation between the effects of enzymatic pretreatment and the intensity of acid hydrolysis.

Materials and methods

Fibers, enzyme and enzymatic treatment

Cotton linters, provided by Celsur (Spain), were used as cellulose source (cellulose content 97.7 ± 0.3 %), and named initial fibers. A cellulase provided by Fungal Bioproducts (Spain) was used for treatments. Activity, as U per gram of enzyme stock was 1700 U/g CMCase units, that is to say, the amount of enzyme degrading 1 μmol of CMC (carboxymethilcellulose) per minute. Enzymatic treatment (C) was performed with a 10 U/g oven-dried pulp (odp) dose for 24h in a 4 L cylindrical reactor with agitation produced by rotating blades at 30 rpm. Treatment was performed at 55 ºC, 5% consistency and pH 5 maintained using 50 mM acetate buffer. Control fibers, named "KC" (0 U/g odp) were obtained using the same conditions as for enzymatic treatment, but without enzymatic adittion.

Experimental designs

The relations existing between process variables for NCC preparation via sulfuric acid hydrolysis and the effects of C were studied via two experimental designs using two different acid concentrations. For this purpose three independent variables were studied: X1 (cellulase) with 0 U/g odp, *i.e.* absence, and 10 U/g odp *i.e.* presence; X2 (acid hydrolysis time) being it 25 or 50 min; X3 (acid hydrolysis temperature) being it 47 ºC or 60 ºC. When the cellulase dose corresponded to "0 U/g odp", we used KC (control fibers) as cellulose source. These independent variables were coded as -1 or +1; both for direct comparison of coefficients and to better understand the effect of each variable on the responses (Table 1). Therefore, the experimental designs were two 2^3 complete factorial designs requiring 8 experiences each. The purpose of this was to only determine individual effects of each of the three variables and their interactions, as described in literature (Valls et al. 2010). Runs in factorial designs were randomized in order to reduce the impact of bias on the results. Data was then analyzed using a Microsoft Excel

129 spreadsheet to implement the stepwise backward regression method and discard all terms
130 with a probability (p-value) less than 0.05 (Table 2).

131 **NCC preparation**

132 Nanocrystalline cellulose was obtained by a controlled hydrolysis via sulfuric acid, using
133 a protocol proposed by Dong et al. 1998. Previous to acid hydrolysis fibers were fluffed
134 and oven-dried. Typically, 1.5 g of fibers weighted immediately from desiccator were
135 hydrolyzed using 62% or 65% wt. sulfuric acid received as 96% PA-ISO (Panreac, Spain)
136 and diluted before use. An acid-to-fibers ratio of 10:1 (10 mL/1g cellulose) was used and
137 reaction was conducted with magnetic stirring. Other reaction conditions were different
138 for each sample and indicated in Table 1. Hydrolysis reaction was quenched using chilled
139 (4ºC) distilled water to dilute samples on a 10-fold basis while cooling them on an ice
140 bath. After this, suspensions were centrifuged at 6000 rpm for 15 min and supernatant
141 was discarded only if not turbid in order to avoid sample loss. Centrifugation step was
142 repeated until supernatant became turbid and not able to be discarded. After
143 centrifugation a sonication step was carried out for NCC dispersion, using a UP100H
144 ultrasonic processor (Hielscher, Germany) at 100% amplitude and 0.75 cycles for 25-30
145 min on an ice bath to prevent heating which is known to be capable of causing desulfation
146 (Dong et al. 1998). Re suspended samples were then dialyzed against distilled water using
147 a 10kDa Thermo Fischer dialysis membrane for three days. After dialysis sonication step
148 was repeated for 20 minutes. Finally, samples were filtered through a Whatman® 41
149 membrane. NCC obtained from cellulase pretreated (presence) and control fibers
150 (absence) was noted as C_NCC and KC_NCC, respectively.

151 **Samples characterization**

152 Cellulose fiber length of initial, control (KC) and cellulase treated (C) fibers was
153 measured in accordance to TAPPI T271 in a Kajaani Fiber analyzer FS300 (Metso
154 automation, Finland).

155 Yield of hydrolysis was determined by drying 25 mL of NCC suspensions at 60 ºC in an
156 air circulating oven and determining NCC mass after water evaporation, a similar
157 procedure to those used by Fan and Li (2012) and Martínez-Sanz et al. (2015). Solids
158 content in suspension was calculated and yield was expressed as % of initial fibers mass.
159 Values were given as average of three independent determinations for each sample.

160 Particle size distribution of samples was determined with dynamic light scattering (DLS)
161 at room temperature (25 ºC) using a particle size analyzer (DL135, Cordouan
162 Technologies, France). NCC suspensions (0.1-0-5% w/v) were placed directly in the
163 measuring cell. Laser power was adjuster for each sample in order to have a count of
164 around 2000 particles/sec. Data was obtained in Cummulants mode and 3 independent
165 measurements were carried out for each sample.

166 NCC surface charge was determined using Mütek particle charge detector (PCD03PH,
167 Mütek, Germany). Suspensions were titrated using a cationic polyelectrolyte (0,001N
168 poly-Dadmac, used as received from Mütek). Surface charge density was calculated
169 according to the following formula:

$$Surface\ charge\ (\frac{meq}{g}) = \frac{VxC}{wt}$$

170 Where V and C are the volume and the concentration of the titration agent (poly-dadmac),
171 respectively, and wt is the weight of the NCC sample.

172 NCC sulfur content was determined according to the procedure described in Abitbol et al.
173 2013. Briefly, a small sample of suspension was titrated using a 1.25 mM NaOH standard
174 solution (Panreac, Spain), recording conductivity values. The equivalence point
175 corresponded to the amount of NaOH necessary to neutralize all the sulfate groups
176 attached to NCC surface. Results were calculated as mass % of atomic sulfur over NCC
177 mass. Values are given as average of three independent measurements for each sample.

178 Electrophoretic mobility of aqueous NCC suspensions (zeta potential) was determined
179 using Zetamaster model *ZEM* (Malvern Instruments, UK). Data was averaged over 12
180 measurements. All samples were analyzed at room temperature.

181 Transmission electron microscopy (TEM) was used to examine NCC morphology using a
182 similar protocol to that described elsewhere (Chen et al. 2015). Carbon-coated Cu-grids
183 were firstly glow-discharged for 30 seconds and then floated on 5 μL drops of NCC
184 suspensions (0.1-0.5 % w/v) for 5 minutes. After that, NCC was negatively stained by
185 floating grids consecutively into two 50 μL drops of 2% aqueous uranyl acetate for 30
186 seconds. Excess stain was removed by capillary action and gentle blotting. Samples were
187 analyzed using a JEOL JEM-1010 transmission electron microscope operating at 80 kV.

188 Fourier transformed infrared spectroscopy (FTIR) spectra of samples was recorded at
189 room temperature using a Spectrum 100 ATR-FTIR spectrophotometer (Perkin Elmer,
190 USA). FTIR spectral analysis was conducted within the wavenumber range of 600-4000
191 cm^{-1}. A total of 64 scans were run to collect each spectrum at a 1 cm^{-1} resolution. Lateral
192 order index (LOI) and Total crystallinity index (TCI), proposed by O'connor (O'Connor
193 et al. 1958) and Nelson and O`Connor (Nelson and O'Connor 1964), were estimated
194 from the ratio between the absorption peaks at 1430 cm^{-1} and 890 cm^{-1} bands, and 1370
195 cm^{-1} and 2900 cm^{-1}, respectively.

196 # Results and discussion

197

198 ### Starting fibers and enzymatic treatment

199 Previous works with the cellulase used in the present study showed that it was capable of
200 substantially reducing fiber length and cellulose viscosity (Quintana et al. 2015a;
201 Beltramino et al. 2015b; Quintana et al. 2015b). Figure 1 showed that cellulase
202 pretreatment modified cotton linters length distribution compared to initial and control
203 fibers, as it reduced the amount of longer fibers (*i.e.* between 3.2 and 7.6 mm) in a 40%,

and increased the amount of shorter ones. Also, a higher homogeneity in fiber length was observed, as more fibers were counted in the middle lengths (groups between 0.5 and 2 mm), highlighting an increase in raw material quality. Control treatment (KC) by its side did not seem to affect fiber length (Figure 1). These macroscopic modifications of fibers together with other chemical modifications such as in viscosity or crystallinity (Beltramino et al. 2015a) are assumed to be the causes of the modifications in acid-fiber interaction during acid hydrolysis produced by enzyme.

Models for yield, average particle size and surface charge

The experimental results obtained for NCC yield, average particle size and surface charge are shown in Table 1. Statistical models were built fitting experimental data, and representative variables showed p-values exposed in Table 2. Yield of the NCC preparation process constitutes a key aspect to be analyzed due to the implication it has on the overall economic cost of the process, as low yields implicate higher biomass and reactants consumption (Klemm et al. 2011; Wang et al. 2012). In this direction, the optimal yield of the process corresponds to the highest possible. Models relating yield for both 62% and 65% wt. H_2SO_4 and other process variables fitted equations 1 and 2, respectively. Eq. 1 shows that yield was positively influenced by cellulase presence (X1), and negatively by reaction time (X2) and temperature (X3), positively by double interaction between time and temperature and negatively by interaction between cellulase and temperature. Eq. 2 indicates that with the stronger acid dose, reaction time did not independently influence yield, but it interacted with cellulase presence and temperature, conditioning their influence.

$$\text{Yield } (\%) = 66.65 + 2.61X1 - 4.82\,X2 - 1.93\,X3 + 5.4\,X2X3 - 1.96X1X3 \quad R^2 = 0.996 \quad \text{(Equation 1)}$$

$$\text{Yield } (\%) = 27.06 + 0.47\,X1 + 0.74\,X3 - 0.51\,X1X2 - 1.24\,X2X3 - 0.23\,X1X2X3$$

$R^2 = 0.999$ (Equation 2)

232 Based on the obtained model, with 62% sulfuric acid yields between 60-84% were
233 obtained (Figure 2a) and cellulase presence increased process outcome up to a ≈9%
234 compared to control fibers (KC), supporting evidence shown by authors in a previous
235 study (Beltramino et al. 2015a). This increase produced by cellulase was speculated to be
236 caused by its preferential attack on amorphous cellulose regions on fibers, increasing their
237 crystallinity and also facilitating the interaction with acid, reducing undesired cellulose
238 mass loss (Beltramino et al. 2015a). Increases in time and temperature reduced hydrolysis
239 yield up to a 20% in cellulase presence, with a smaller effect on its absence. Yields with
240 65% acid were smaller compared to 62% H_2SO_4, with values among 24-30%,
241 consequence of the stronger depolymerization of cellulose produced by a larger acid
242 concentration (Chen et al. 2015). Even in these conditions, cellulase showed to be capable
243 of increasing yield up to ≈2.4%, strongly highlighting the benefits of this pretreatment.
244 With this stronger acid dose (65%), time and temperature had little influence in yield.

245 Concerning average particle size, generally, DLS measurements do not provide a real
246 measurement of particle size, particularly when considering rod-like structures such as
247 nanocrystalline cellulose (Fraschini et al. 2014). Nevertheless, these measurements
248 provide a useful approximation to average particle size in order to establish comparisons
249 between similar samples (Fraschini et al. 2014). Size of nanocrystalline cellulose is a key
250 aspect to analyze in order to ensure the quality and characteristics of the obtained final
251 product (Fraschini et al. 2014), as NCC morphology could affect their performance when
252 used on a determined application. These affectations could be, for instance, variations in
253 permeability of membranes formed by NCC (Thielemans et al. 2009) or toxicity, as it has
254 been found that smaller NCC particles showed greater toxicity than larger ones
255 (Yanamala and Farcas 2014). Also, we previously reported that size of NCC and their
256 yield seemed to be related parameters (Beltramino et al. 2015a). Equations 3 and 4
257 indicate the models fitting Z average values with 62% and 65% wt. H_2SO_4, respectively.
258 For 62% acid, we observed that particle size was only affected (negatively) by reaction
259 time and temperature and positively by their double interaction. Similar influences were

found for 65% acid, although in this case, cellulase positively influenced this parameter, as well as it interacted with both time and temperature.

With 62% sulfuric acid (Figure 2c) we found that particle size was statistically not influenced by cellulase presence. However, data in Table 1 suggested that cellulase pretreatment could increase NCC particle size, as observed in a previous work (Beltramino et al. 2015a). Reaction time and temperature both reduced average particle up to a 60%, as they enhanced cellulose degradation. With 65% acid (Figure 2d), average particle size was strongly reduced, consequence of the greater cellulose depolymerization produced by acid, as observed by other authors (Fan and Li 2012). With this stronger acid dose, cellulase presence increased particle size up to 15nm, while reaction time and temperature reduced size particularly in absence of enzymatic pretreatment.

$$\text{Z average (nm)} = 112.7 - 26.2\,X2 - 36.2\,X3 + 24.5\,X2X3 \quad R^2 = 0.976 \quad \text{(Equation 3)}$$

$$\text{Z average (nm)} = 82.4 + 4.8\,X1 - 1.6\,X2 - 6.8\,X3 + 1.9\,X1X2 + 1.1\,X1X3 \quad R^2 = 0.998 \quad \text{(Equation 4)}$$

Surface charge of cellulose NCC is mainly responsibility of sulfate groups esterified onto free superficial OH- groups of cellulose during hydrolysis with sulfuric acid (Habibi et al. 2010; Abitbol et al. 2013). Because of this, NCC obtained with different acids, such as hydrochloric or hydrobromic result mainly uncharged (Habibi et al. 2010). Thus, NCC surface charge and their sulfur content are expected to be related. Equations 5 and 6 fitted surface charge data for 62% and 65% wt. acid, respectively. In the first case, surface charge showed to be positively influenced by reaction time and temperature, and negatively by interaction of cellulase and temperature. In the second case influences were different, with cellulase reducing surface charge and interacting with the other two variables.

Surface charge (meq/g) $= 0.224 + 0.014\ X2 + 0.033\ X3 - 0.012\ X1X3 \quad R^2 = 0.956$ (Equation 5)

Surface charge (meq/g) $= 0.223 - 0.01\ X1 + 0.004\ X3 - 0.01\ X1X2 + 0.007\ X1X3 \quad R^2 = 0.980$ (Equation 6)

NCC surface charge increased with time and temperature with 62% wt. sulfuric acid (Figure 2e), probably consequence of higher levels of sulfate esterification at higher temperatures or longer hydrolysis times, as also observed by Chen et al. (2015). At this acid concentration, cellulase effect was found to depend on temperature. With 65% wt. sulfuric acid, C_NCC showed a lower surface charge compared to KC_NCC, possibly consequence of a lower sulfate esterification. Also, only little influence seemed to be caused by hydrolysis time and temperature on surface charge with the stronger acid dose, the same happening for NCC yield and particle size.

Table 1: Experiences of both statistical plans with their conditions and obtained experimental values.

Sulfuric acid 62% wt.									
	X1	X2	X3	Cellulase (U/g odp)	Time (min)	Temperature (ºC)	Yield (%)	Z average (nm)	Surface charge (meq/g)
Y1	-1	-1	-1	0	25	47	73.5 ± 0.2	184.8 ± 5.6	0.164 ± 0.02
Y2	1	-1	-1	10	25	47	84.1 ± 0.5	214.7 ± 34.3	0.188 ± 0.009
Y3	-1	1	-1	0	50	47	54.5 ± 0.3	97.5 ± 1	0.190 ± 0.002
Y4	1	1	-1	10	50	47	62.2 ± 0.2	98.9 ± 2.8	0.222 ± 0.001
Y5	-1	-1	1	0	25	60	63.3 ± 0.2	76.7 ± 1.2	0.265 ± 0.014
Y6	1	-1	1	10	25	60	64.9 ± 0.2	79.7 ± 2.3	0.225 ± 0.013
Y7	-1	1	1	0	50	60	64.8 ± 0.5	69.3 ± 2.3	0.269 ± 0.008
Y8	1	1	1	10	50	60	65.8 ± 0.5	80.2 ± 2	0.271 ± 0.016
Sulfuric acid 65% wt.									
	X1	X2	X3	Cellulase (U/g odp)	Time (min)	Temperature (ºC)	Yield (%)	Z average (nm)	Surface charge (meq/g)
Y1	-1	-1	-1	0	25	47	24.4 ± 0.1	89.2 ± 1.6	0.227 ± 0.005
Y2	1	-1	-1	10	25	47	25.8 ± 0.6	92.3 ± 3.6	0.216 ± 0.009
Y3	-1	1	-1	0	50	47	27.4 ± 0.4	81.6 ± 5.7	0.245 ± 0.01
Y4	1	1	-1	10	50	47	27.7 ± 0.3	93.4 ± 1.9	0.188 ± 0.011
Y5	-1	-1	1	0	25	60	27.8 ± 0.2	72.6 ± 0.6	0.222 ± 0.01

Y6	1	-1	1	10	25	60	30.3 ± 0.3	81.5 ± 1.4	0.232 ± 0.011
Y7	-1	1	1	0	50	60	26.8 ± 0.2	66.6 ± 1.6	0.241 ± 0.004
Y8	1	1	1	10	50	60	26.3 ± 0.4	81.6 ± 1.5	0.216 ± 0.014

300

301 Table 2: p-values of each variable for the different obtained models using each acid dose.

	Yield		Z average		Surface charge	
	62 % wt.	65 % wt.	62 % wt.	65 % wt.	62 % wt.	65 % wt.
X1	0.0196	0.0055	-	0.0024	-	0.0047
X2	0.0059	-	0.0014	0.0231	0.0269	-
X3	0.0352	0.0022	0.0005	0.0012	0.0012	0.0490
X1X2	-	0.0047	-	0.0164		0.0054
X1X3	0.0339	-	-	0.0433	0.0440	0.0161
X2X3	0.0047	0.0008	0.0018	-	-	-
X1X2X3	-	0.0219	-	-	-	-

302

303

304 **NCC sulfur content, stability and polydispersity**

305 Sulfate groups could influence several characteristics of NCC, such as their dispersibility
306 in water suspensions (Klemm et al. 2011) or their thermodegradability (Roman and
307 Winter 2004). They could also influence the properties they could confer to composites if
308 used as fillers (Moon et al. 2011). Sulfate groups on crystals surface would allow their
309 use in biomedical applications, due to the possibility of electrostatically absorb enzymes
310 or proteins (Lin and Dufresne 2014). NCC with no SO_4^{2-} groups on its surface, such as
311 those obtained with enzymes (Filson et al. 2009; Anderson et al. 2014; Teixeira et al.
312 2015) or non-sulfuric acids (*e.g.* hydrobromic or hydrochloric) (Habibi et al. 2010)
313 aggregate and flocculate on water, hindering their applicability. NCC with large contents
314 in sulfur, on the other hand, would be very susceptible to thermal degradation (Roman
315 and Winter 2004), hindering their use as fillers in polymeric matrixes, which are usually
316 manipulated at high temperatures (Hubbe et al. 2008). Sulfur content of samples are
317 indicated in Figure 3. In it, it can be observed, firstly that the larger acid concentration led
318 to higher content in sulfurs, result of the larger extent of esterification, as previously
319 reported in literature (Beltramino et al. 2015a; Chen et al. 2015). Secondly, cellulase

influence on NCC sulfation was found to depend upon other conditions. Generally, we observed that it seemed to produce an opposite effect at lower and higher acid concentrations, seeming to reduce sulfation in the former and increasing it in the latter. Lastly, concerning hydrolysis time and temperature, no remarkable influence was found with 62% wt. acid, while with 65% wt. acid they showed to reduce NCC sulfur content when increased. This observed desulfation was attributed to the degradation of NCC to sugars due to excessive depolymerization (Chen et al. 2015).

Zeta potential, measured as electrophoretic mobility, is an indicator the stability of colloidal suspensions (Filson et al. 2009; Alves et al. 2014). As indicated in Figure 4a, all the studied hydrolysis conditions led to values between -45 mV and -60 mV, considered to be indicators of very high stability (Alves et al. 2014). Little differences were found among samples, only being able to observe an increase in stability by increasing hydrolysis severity. These results indicated that well stable NCC suspensions were obtained independently of conditions and highlighting another benefit of using combined treatments with enzymes and sulfuric acid hydrolysis.

Polydispersity index (PDI) is a measure of the heterogeneity in particle sizes within a sample, where smaller values indicate a higher homogeneity. It is known that having a NCC sample with a high homogeneity in particle size, *i.e.* a narrow particle size distribution is an indicator of good quality (Moon et al. 2011) and thereafter a desirable feature. Also, this homogeneity constitutes a necessary feature for NCC application as a standardized component (Moon et al. 2011). As illustrated (Figure 4b), all samples had PDI values around 0.2 indicating samples particle size distribution was homogeneous.

Optimal point and model verification

The objective of the present work was to find the hydrolysis conditions producing the highest possible NCC yield. Thus, the optimal point was defined as the one providing the maximal yield. From the obtained statistical models, we found these conditions to be:

cellulase presence (X1 = 1), 25 minutes of hydrolysis (X2 = -1) and 47 ºC (X3 = -1). At these conditions a yield of 83.4% was predicted by model. These conditions also provided also a maximal yield value of 74.2% in absence of cellulase, which was smaller than the former and thereafter considerably less interesting. Comparing these conditions with those used on previous studies (Beltramino et al. 2015a) it can be noticed that a reduction of 20 min, *i.e.* 44% in acid hydrolysis time was achieved. Also, these optimized conditions led to a yield more than 10% higher than that obtained in the previous work, possibly by reducing unnecessary cellulose depolymerization.

Optimal yield was also significantly higher than other reported values. Recently, Fan and Li 2012 reported a ≈62% optimal yield from cotton fibers and Martínez-Sanz et al. 2014 reported ≈77% yield for NCC also derived from pure cellulosic sources, both using a similar procedure for yield measurement. Other innovative preparation methods such as ultrasonic assisted hydrolysis (Tanaka et al. 2014) offered a ≈40% yield. At optimal conditions, models also predicted the larger NCC size among those observed, around 200 nm, fact that would reduce their toxicity (Yanamala and Farcas 2014). Also, at this point surface charge was among the lower ones, indirectly indicating a low sulfate presence on NCC surface which would reduce their thermodegradability (Roman and Winter 2004). Finally, zeta potential and polydispersity index provided evidence that optimal point provided a sample with high stability and a narrow size distribution. In order to check the accuracy of the obtained models, new samples were prepared using the optimal hydrolysis conditions in presence and absence of cellulase.

Table 3 indicates these new experimental values and also those predicted by models. As can be observed, models successfully predicted experimental data for yield, surface charge and average size within confidence intervals, only observing a small bias in the latter (<5 nm). Concerning non-modelized parameters, new values were also similar to former ones, with only small discrepancies in parameters showing a higher variability among samples, such as sulfur content or zeta potential.

374 Table 3: Models verification. New experimental values and those predicted by models are
375 indicated for optimal hydrolysis conditions (25 min, 47 ºC and sulfuric acid 62% wt.). *When no
376 model was found fitting data, previous experimental value is indicated.

	Optimal conditions			
	10 U/g odp cellulase		0 U/g odp cellulase	
	Experimental	Predicted*	Experimental	Predicted*
Yield (%)	82.8 ± 1.1	83.4	72.4 ± 1.2	74.2
Z average (nm)	186.4 ± 9.5	199.6	174.2 ± 19.1	199.6
Surface charge (meq/g)	0.185 ± 0.02	0.165	0.180 ± 0.018	0.189
Sulfur content (% S)	0.82 ± 0.04	1.1 ± 0.21	0.93 ± 0.03	1.21 ± 0.3
Zeta potential (mV)	-49.6 ± 1.1	-50.1 ± 1.1	-49.8 ± 0.8	-45 ± 2.6
PDI	0.17 ± 0.02	0.20 ± 0.03	0.19 ± 0.03	0.19 ± 0.02

377

378 **TEM analysis**

379 Transmission electron microscope (TEM) images of individual NCC particles are shown
380 in Figure 5. Firstly, images confirmed the achievement of rod-shaped nanostructures
381 (NCC) at optimal and also at other studied conditions. Secondly, agreeing with DLS data,
382 images of NCC obtained with optimal conditions in presence and absence of cellulase
383 pretreatment (Figure 5a and b) seemed to show the largest particles, not observing
384 noticeable differences between both samples. Images in Figure 5c, d and e by their side
385 seemed to expose NCC particles with a smaller size compared to the former ones. This
386 evidence was predicted by DLS data and was explained by the stronger hydrolysis
387 severity caused either by longer hydrolysis, a higher temperature or a higher acid
388 concentration, as previously exposed.

389

390 **FTIR analysis**

391 On Figure 6 examples of FTIR spectra of cellulose fibers and extracted NCC are shown.
392 In the three cases spectra appeared to be very similar, attending the fact that chemical
393 composition of samples (pure cellulose) remained unchanged during all studied
394 processes. Main differences found were related to peaks intensity. Typical bands of
395 cellulose were observed (Široký et al. 2010). The broad absorption band in the range of
396 3600-3100 cm^{-1} was mainly due to the stretching of the –OH groups of cellulose, with

typical sharpening around 3400 cm^{-1} (Široký et al. 2010; Alves et al. 2014). The peak at 2900 cm^{-1} appeared due to C-H stretching of cellulose (Fahma et al. 2010). Band at 1650-1600 cm^{-1} originated from the bending mode of water absorbed on cellulose (*i.e.* moisture water) (Fahma et al. 2010). From 1800 to 600 cm^{-1} the anhydroglucopyranose vibration modes were shown (deformation, wagging and twisting) (Alves et al. 2014). Among them, the absorption at 1044 cm^{-1} was mainly attributed to C-O stretching on C-O-C linkages, and the band at 895 cm^{-1} to C-H deformation of β-glyosidic linkages between glucose units (Alves et al. 2014). Presence of sulfate groups on NCC, not present on original fibers is illustrated by a small peak at 1205 cm^{-1}, which can be attributed to S=O linkage vibration, as previously described (Lu and Hsieh 2010; Flauzino Neto et al. 2013). This tiny peak appears at NCC samples spectra but seems to be inexistent at original fibers (Figure 6).

It has been reported that segments in cellulose polymer will vibrate differently in well-ordered crystalline regions compared to amorphous phases, permitting then the assignation of absorption bands to crystalline and amorphous regions and allowing the calculation of two different crystallinity indexes. Lateral Order Index (LOI), being the absorption ratio of bands at 1430 cm^{-1} (characteristic of crystalline areas) and 890 cm^{-1} band (representing amorphous regions) is correlated to overall degree of order in cellulose (O'Connor et al. 1958). Total Crystallinity Index (TCI), by its side, is calculated from the ratio of absorption peaks at 1370 and 2900 cm^{-1} and claimed to be proportional to cellulose crystallinity index (Nelson and O'Connor 1964). Cellulose crystallinity determination is important due to its impact on cellulose practical characteristics. Crystallinity index is determined by the proportion between crystalline and amorphous regions, while is also affected by the different possible spatial arrangements of the polymer (French and Santiago Cintrón 2013). Likewise, cellulose crystallinity index has been related to the size of crystalline domains (French and Santiago Cintrón 2013), matter of great importance when considering NCC preparation. In Table 4 values for TCI and LOI of fibers and NCC samples are indicated. Concerning fibers it can be seen how TCI

increased after enzymatic treatment, suggesting an increase in fiber crystallinity, possibly consequence of cellulase preferential attack on amorphous regions (Ahola et al. 2008). The decrease in the other studied index (LOI) in fibers, consequence of enzyme action, meaning a reduction in the overall order degree of cellulose, could be related to an increase in accessibility to cellulose surface (Spiridon et al. 2010). This modification in LOI value was consistent previous observations, and could help explaining the improved outcome of sulfuric acid hydrolysis of enzymatically pretreated fibers compared to untreated. Regarding NCC (Table 4) firstly, we observed TCI increasing in all samples compared to their original fibers, consequence of amorphous regions removal during acid hydrolysis. Secondly, we observed that the larger cellulose depolymerization produced by the greatest acid dose reduced TCI values of NCC, probably because of the notorious reduction in crystals size (French and Santiago Cintrón 2013). Lastly, cellulase pretreatment increased TCI of NCC, possibly due to a larger presence of crystalline cellulose in NCC and/or a size increase of these regions. FTIR data suggested that a more accessible and crystalline cellulose structure was obtained on cellulose fibers as a consequence of cellulase action. These modifications might have produced a cleaner and more rapid access of sulfuric acid to more abundant crystalline regions, reducing sample loss on the acid hydrolysis process and providing larger NCC particles with a higher crystallinity. This evidence was also in accordance with the proposed mechanism underlying the NCC yield increase produced by cellulase.

Table 4: Total crystallinity index (TCI) and Lateral order index (LOI) of fibers and NCC. Data for NCC was obtained at 25 minutes and 60 ºC.

	Cellulose fibers		NCC			
Cellulase dose	0 U/g odp	10 U/g odp	0 U/g odp		10 U/g odp	
Acid dose	-	-	62%	65%	62%	65%
TCI	0.69	0.92	1.46	0.79	2.01	1.29
LOI	1.02	0.67	0.33	0.31	0.36	0.5

Conclusions

Results presented in this work allowed us to find the optimal chemical conditions maximizing yield for NCC isolation from enzymatically pre-treated fibers, obtaining yields higher than 80% and with an enzyme-aided gain of 9%. Also, this optimization permitted to substantially reduce hydrolysis time (a 44%), and increasing yield in more than 10% compared to the conditions used in a previous work. We found that at optimal conditions particle size was still on nano-scale and surface charge was reduced, the same that happened with sulfur content. Results also indicated that all samples suspensions had good stability values and a narrow particle size distribution. Cellulase effects were noticeable even with a large acid concentration, highlighting the potential of this pretreatment. TEM analysis confirmed the presence of NCC even under the milder hydrolysis conditions and FTIR measurements indicated that cellulase treatments increased fibers and NCC crystallinity and also accessibility to fibers. The conditions found in this study will permit a better usage of raw materials for NCC production, reducing unnecessary biomass consumption and maintaining product quality.

Acknowledgments

Authors are grateful to "Ministerio de Economía y Competitividad" (Spain) for their support in this work under the BIOSURFACEL (CTQ2012-34109, funding also from the "Fondo Europeo de Desarrollo Regional, FEDER") and BIOPAPµFLUID (CTQ2013-48995-C2-1-R) projects and a FPI grant (BES-2011-046674). Special thanks are also due to the consolidated research group AGAUR 2014 SGR 534 with Universitat de Barcelona (UB). We are also grateful to Celsur and Fungal Bioproducts for supplying cotton linters and enzyme, respectively.

References

Abitbol T, Kloser E, Gray DG (2013) Estimation of the surface sulfur content of cellulose nanocrystals prepared by sulfuric acid hydrolysis. Cellulose 20:785–794.

Ahola S, Turon X, Osterberg M, et al (2008) Enzymatic hydrolysis of native cellulose nanofibrils and other cellulose model films: effect of surface structure. Langmuir 24:11592–9. doi: 10.1021/la801550j

Alves L, Medronho B, Antunes FE, et al (2014) Unusual extraction and characterization of nanocrystalline cellulose from cellulose derivatives. J Mol Liq. doi: 10.1016/j.molliq.2014.12.010

Anderson SR, Esposito D, Gillette W, et al (2014) Enzymatic preparation of nanocrystalline and microcrystalline cellulose. Tappi J 13:35–42.

485 Beltramino F, Roncero MB, Vidal T, et al (2015a) Increasing yield of nanocrystalline cellulose
486 preparation process by a cellulase pretreatment. Bioresour Technol 192:574–581. doi:
487 10.1016/j.biortech.2015.06.007

488 Beltramino F, Valls C, Vidal T, Roncero MB (2015b) Exploring the effects of treatments with
489 carbohydrases to obtain a high-cellulose content pulp from a non-wood alkaline pulp.
490 Carbohydr Polym 133:302 – 312. doi: 10.1016/j.carbpol.2015.07.016

491 Brinchi L, Cotana F, Fortunati E, Kenny JM (2013) Production of nanocrystalline cellulose from
492 lignocellulosic biomass: Technology and applications. Carbohydr Polym 94:154–169. doi:
493 http://dx.doi.org/10.1016/j.carbpol.2013.01.033

494 Chen L, Wang Q, Hirth K, et al (2015) Tailoring the yield and characteristics of wood cellulose
495 nanocrystals (CNC) using concentrated acid hydrolysis. Cellulose. doi: 10.1007/s10570-015-
496 0615-1

497 Dong XM, Revol J-F, Gray DG (1998) Effect of microcrystallite preparation conditions on the
498 formation of colloid crystals of cellulose. Cellulose 5:19–32.

499 Fahma F, Iwamoto S, Hori N, et al (2010) Isolation, preparation, and characterization of
500 nanofibers from oil palm empty-fruit-bunch (OPEFB). Cellulose 17:977–985. doi:
501 10.1007/s10570-010-9436-4

502 Fan JS, Li YH (2012) Maximizing the yield of nanocrystalline cellulose from cotton pulp fiber.
503 Carbohydr Polym 88:1184–1188. doi: 10.1016/j.carbpol.2012.01.081

504 Filson PB, Dawson-Andoh BE, Schwegler-Berry D (2009) Enzymatic-mediated production of
505 cellulose nanocrystals from recycled pulp. Green Chem 11:1808. doi: 10.1039/b915746h

506 Flauzino Neto WP, Silvério HA, Dantas NO, Pasquini D (2013) Extraction and characterization of
507 cellulose nanocrystals from agro-industrial residue - Soy hulls. Ind Crops Prod 42:480–488.
508 doi: 10.1016/j.indcrop.2012.06.041

509 Fraschini C, Chauve G, Berre J-F Le, et al (2014) Critical discussion of light scattering and
510 microscopy techniques for CNC particle sizing. Nord Pulp Pap Res J 29:31–40.

511 French AD, Santiago Cintrón M (2013) Cellulose polymorphy, crystallite size, and the Segal
512 Crystallinity Index. Cellulose 20:583–588. doi: 10.1007/s10570-012-9833-y

513 Habibi Y, Lucia LA, Rojas OJ (2010) Cellulose nanocrystals: Chemistry, self-assembly, and
514 applications. Chem Rev 110:3479–3500. doi: 10.1021/cr900339w

515 Hubbe MA, Rojas OJ, Lucia LA, Sain M (2008) Cellulosic nanocomposites: a review. BioResources
516 3:929–980.

517 Klemm D, Kramer F, Moritz S, et al (2011) Nanocelluloses: A new family of nature-based
518 materials. Angew Chemie - Int Ed 50:5438–5466. doi: 10.1002/anie.201001273

519 Lin N, Dufresne A (2014) Nanocellulose in biomedicine: Current status and future prospect. Eur
520 Polym J 59:302–325. doi: 10.1016/j.eurpolymj.2014.07.025

521 Lu P, Hsieh Y-L (2010) Preparation and properties of cellulose nanocrystals: Rods, spheres, and
522 network. Carbohydr Polym 82:329–336. doi:
523 http://dx.doi.org/10.1016/j.carbpol.2010.04.073

524 Martínez-Sanz M, Vicente AA, Gontard N, et al (2015) On the extraction of cellulose
525 nanowhiskers from food by-products and their comparative reinforcing effect on a
526 polyhydroxybutyrate-co-valerate polymer. Cellulose 22:535–551. doi: 10.1007/s10570-014-
527 0509-7

528 Moon RJ, Martini A, Nairn J, et al (2011) Cellulose nanomaterials review: structure, properties
529 and nanocomposites. Chem Soc Rev 40:3941–94. doi: 10.1039/c0cs00108b

530 Nelson ML, O'Connor RT (1964) Relation of certain infrared bands to cellulose crystallinity and
531 crystal lattice type. Part II. A new infrared ratio for estimation of crystallinity in celluloses I

and II. J Appl Polym Sci 8:1325–1341. doi: 10.1002/app.1964.070080323

O'Connor RT, DuPré EF, Mitcham D (1958) Applications of Infrared Absorption Spectroscopy to Investigations of Cotton and Modified Cottons Part I: Physical and Crystalline Modifications and Oxidation. Text Res J 28:382–392. doi: 10.1177/004051755802800503

Quintana E, Valls C, Vidal T, Roncero MB (2015a) Comparative evaluation of the action of two different endoglucanases. Part II: On a biobleached acid sulphite pulp. Cellulose 22:2081–2093. doi: 10.1007/s10570-015-0631-1

Quintana E, Valls C, Vidal T, Roncero MB (2015b) Comparative evaluation of the action of two different endoglucanases. Part I: On a fully bleached, commercial acid sulfite dissolving pulp. Cellulose 2067–2079. doi: 10.1007/s10570-015-0623-1

Roman M, Winter WT (2004) Effect of sulfate groups from sulfuric acid hydrolysis on the thermal degradation behavior of bacterial cellulose. Biomacromolecules 5:1671–7. doi: 10.1021/bm034519+

Široký J, Blackburn RS, Bechtold T, et al (2010) Attenuated total reflectance Fourier-transform Infrared spectroscopy analysis of crystallinity changes in lyocell following continuous treatment with sodium hydroxide. Cellulose 17:103–115. doi: 10.1007/s10570-009-9378-x

Spiridon I, Teaca C-A, Bodîrlau R (2010) Structural Changes Evidenced By Ftir Pre-Treatment With Ionic Liquid and Enzymatic. BioResources 6:400–413.

Tanaka R, Saito T, Ishii D, Isogai A (2014) Determination of nanocellulose fibril length by shear viscosity measurement. Cellulose 21:1581–1589. doi: 10.1007/s10570-014-0196-4

Teixeira RSS, Silva AS Da, Jang J-H, et al (2015) Combining biomass wet disk milling and endoglucanase/β-glucosidase hydrolysis for the production of cellulose nanocrystals. Carbohydr Polym 128:75–81. doi: 10.1016/j.carbpol.2015.03.087

Thielemans W, Warbey CR, Walsh D a. (2009) Permselective nanostructured membranes based on cellulose nanowhiskers. Green Chem 11:531 – 537. doi: 10.1039/b818056c

Valls C, Colom JF, Baffert C, et al (2010) Comparing the efficiency of the laccase–NHA and laccase–HBT systems in eucalyptus pulp bleaching. Biochem Eng J 49:401–407. doi: 10.1016/j.bej.2010.02.002

Valls C, Roncero MB (2009) Using both xylanase and laccase enzymes for pulp bleaching. Bioresour Technol 100:2032–9. doi: 10.1016/j.biortech.2008.10.009

Wang QQ, Zhu JY, Reiner RS, et al (2012) Approaching zero cellulose loss in cellulose nanocrystal (CNC) production: recovery and characterization of cellulosic solid residues (CSR) and CNC. Cellulose 19:2033–2047. doi: 10.1007/s10570-012-9765-6

Yanamala N, Farcas M (2014) In vivo Evaluation of the Pulmonary Toxicity of Cellulose Nanocrystals: A Renewable and Sustainable Nanomaterial of the Future. ACS Sustain Chem Eng 2:1691 – 1698.

Figure Captions

Figure 1: Fiber length (mm) distribution of initial, cellulase treated (C) and control (KC) fibers indicated as % of total.

Figure 2: Data predicted by models with 62% wt. sulfuric acid: Yield (a), average size (c) and surface charge (e); and with 65% wt. sulfuric acid: Yield (b), average size (d), surface charge (f). Grey and black charts represent data in presence and absence of cellulase, respectively.

Figure 3: Sulfur content (as % S) of samples at studied conditions in presence and absence of cellulase.

Figure 4: Zeta Potential (a) and Polydispersity Index (PDI) (b) of samples at studied conditions in presence and absence of cellulase

Figure 5: TEM images of NCC. Images correspond to: cellulase, 25 min, 47 ºC 62% acid (optimal point, A); control, 25 min, 47 ºC, 62% acid (B); cellulase, 50 min, 60ºC, 62% acid (C); cellulase, 25 min, 47 ºC, 65% acid (D); cellulase, 50 min, 47 ºC, 65% acid (E). Scale bar: 100 nm.

Figure 6: FTIR spectra of C24 fibers (a), NCC (no cellulase, 62% wt. acid, 25 min) (b), NCC (cellulase, 65% wt. acid, 50 min) (c).

Figure 1:

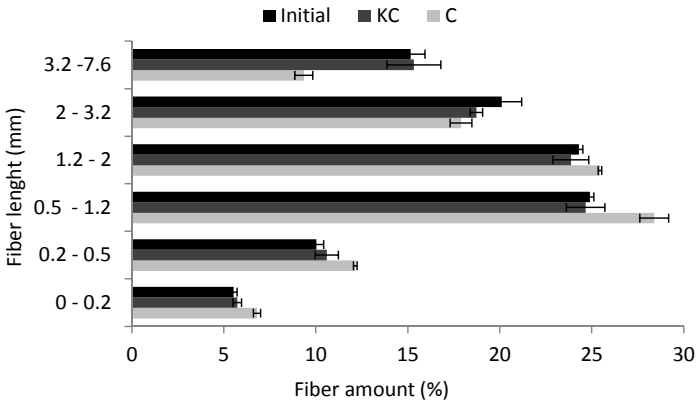

Figure 2:

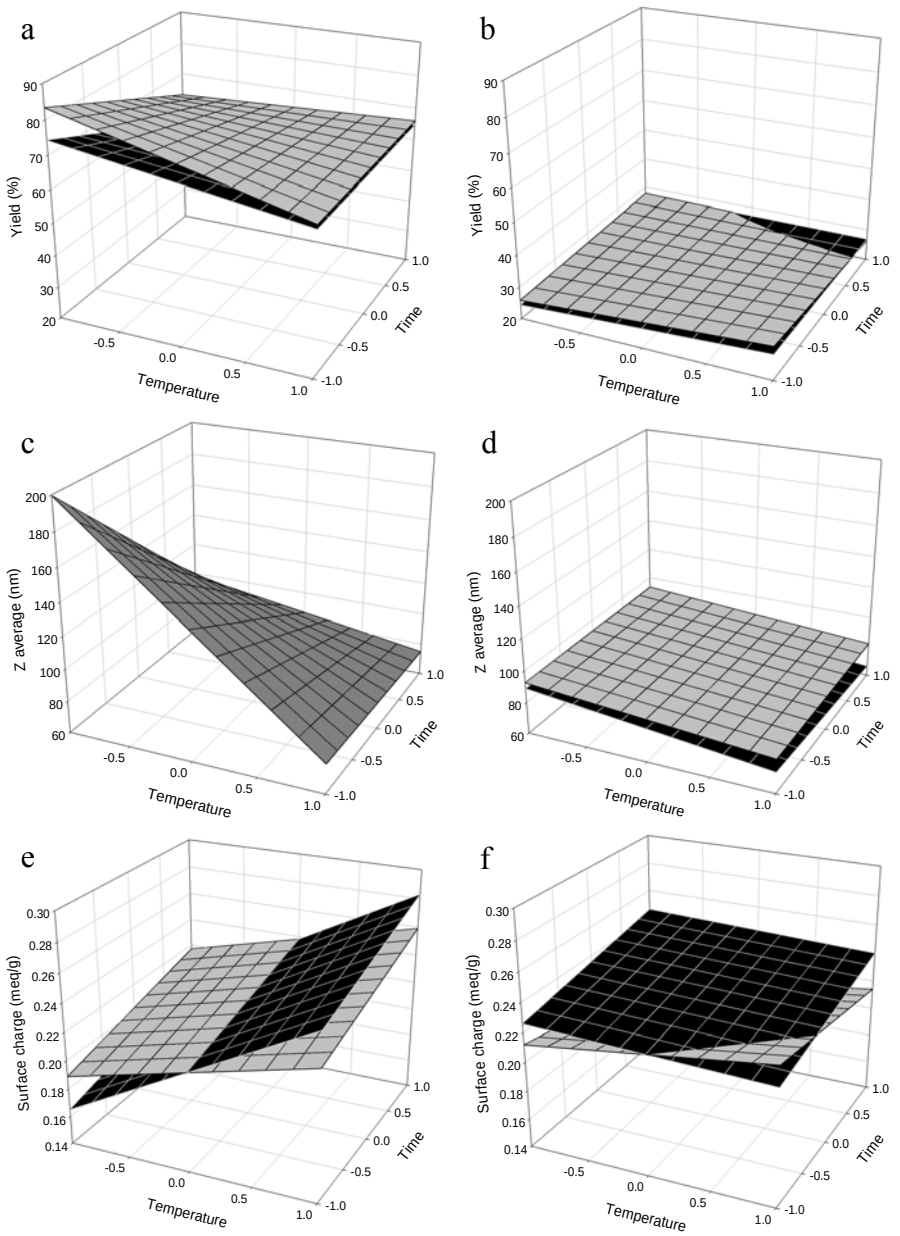
a
Yield (%)
90
80
70
60
50
40
30
20
-0.5
0.0
0.5
1.0
Temperature
1.0
0.5
0.0
-0.5
-1.0
Time
b
Yield (%)
Temperature
Time
c
Z average (nm)
200
180
160
140
120
100
80
60
Temperature
Time
d
Z average (nm)
Temperature
Time
e
Surface charge (meq/g)
0.30
0.28
0.26
0.24
0.22
0.20
0.18
0.16
0.14
Temperature
Time
f
Surface charge (meq/g)
Temperature
Time

Figure 3:

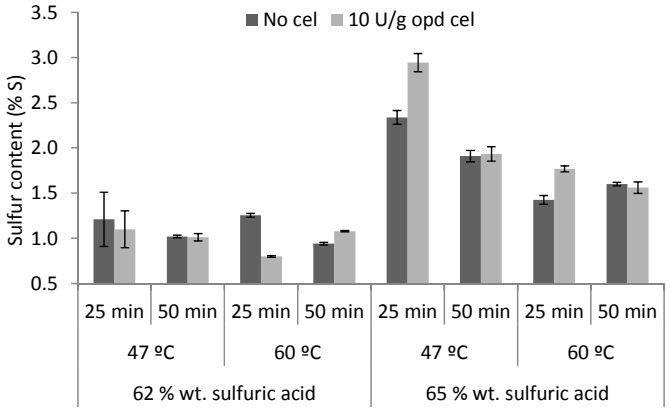

Figure 4:

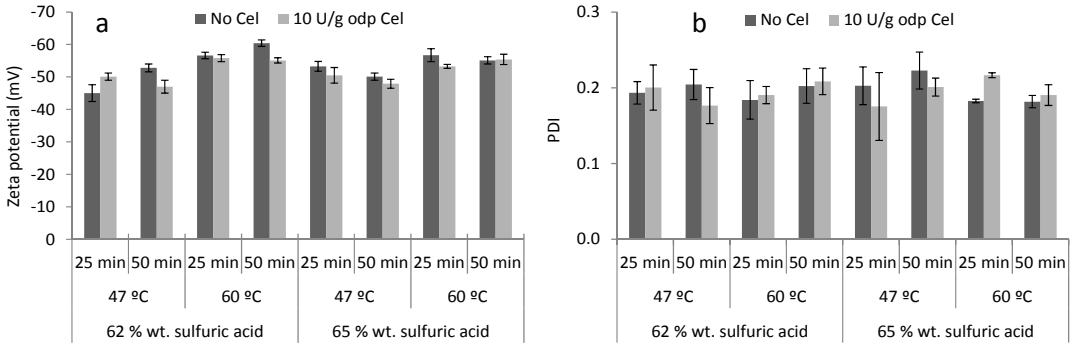

627 Figure 5:

628

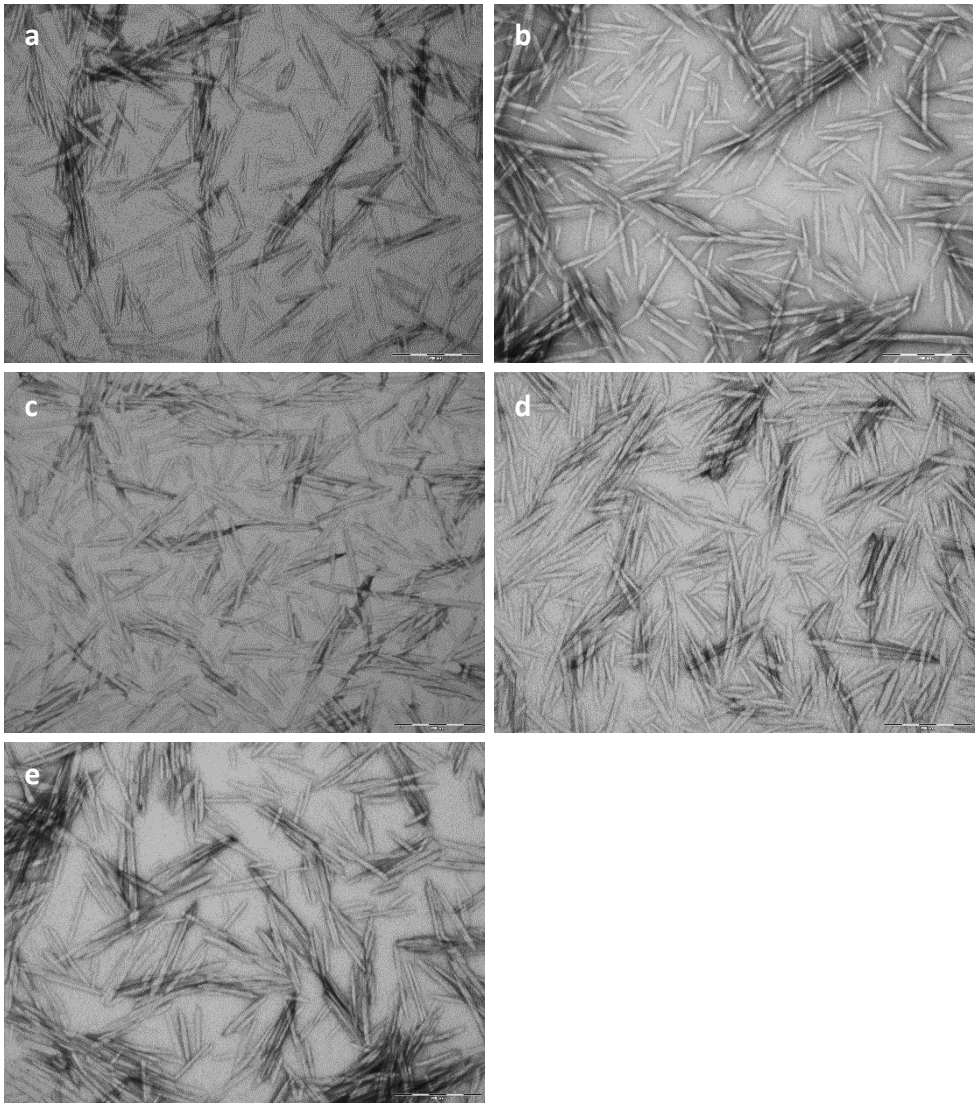

629
630

631 Figure 6:

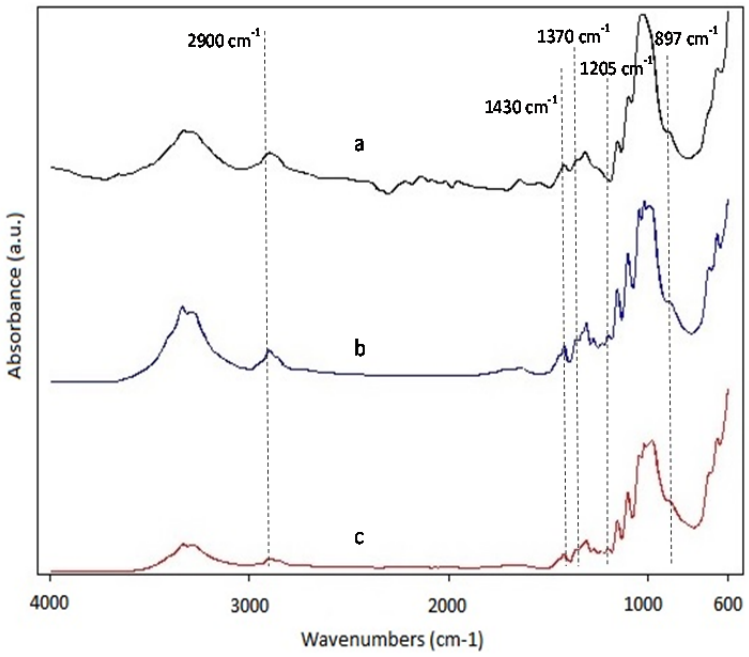

632

633